Hindawi Publishing Corporation
International Journal of Antennas and Propagation
Volume 2013, Article ID 837643, 8 pages
http://dx.doi.org/10.1155/2013/837643

*Research Article*

# Design of a Compact MIMO Antenna Using Coupled Feed for LTE Mobile Applications

**Xing Zhao, Youngki Lee, and Jaehoon Choi**

*Department of Electronics and Communications Engineering, Hanyang University, 17 Haengdang-dong, Seongdong-gu, Seoul 133-791, Republic of Korea*

Correspondence should be addressed to Jaehoon Choi; choijh@hanyang.ac.kr

Received 10 September 2012; Revised 31 December 2012; Accepted 1 January 2013

Academic Editor: Hon Tat Hui



A compact multi-input multi-output (MIMO) antenna with a coupled feed structure for 4th generation (4G) handsets is proposed for operation in long-term evolution (LTE) band 13 (0.746 GHz–0.787 GHz). The MIMO antenna consists of two symmetrically distributed identical antenna elements. The size of each element is limited to 20 mm × 10 mm × 5 mm ($\lambda_0$ = 392 mm at 0.765 GHz), and the separation between different elements is minimized to 15 mm. Each antenna element contains a Z-shaped coupled feed strip and a simple folded monopole-type radiating element. The simple folded radiating element supports two monopole modes (first order) excited at adjacent frequencies to achieve broadband performance. The coupled feed strip effectively modifies impedance matching and maintains good isolation. The proposed antenna has a 6 dB return loss bandwidth of 55 MHz (0.735 GHz–0.79 GHz) and isolation above 12 dB without the use of an additional isolation enhancement element. Moreover, the envelope correlation coefficient (ECC) is maintained below 0.5 over the designed frequency band.

## 1. Introduction

Long-term evolution (LTE) is considered to be one of the most progressive 4G mobile standards to increase the channel capacity and speed of mobile handset networks [1]. Major mobile terminal manufacturers around the world, including Samsung, LG, and Apple, have devoted extensive research to the development of LTE handsets so as to guarantee an early lead in the field and maintain shares in the future market. This new trend in LTE handsets brings significant opportunities and challenges to antenna engineers.

Multi-input multi-output (MIMO) antennas are expected to support LTE wireless communication systems [2]. When a MIMO antenna is installed in a handset, at least two uncorrelated antenna elements should be compressed into an extremely restricted space. This task becomes especially challenging when the MIMO antenna is designed for LTE band 13 (corresponding wavelength of 390 mm). Due to the limited space available for antenna elements, the elements are strongly coupled with each other, and narrow bandwidth characteristics are induced. Moreover, since two antenna elements are located on the same ground plane, the current distribution, especially around feed ports, would affect the isolation [3].

To overcome this problem, compact broadband antenna elements suitable for mobile MIMO antenna systems are needed. Some compact broadband antennas with functional frequency bands located between 0.5 GHz and 1 GHz have been proposed for mobile applications [4–7]. However, isolation is usually low when these antennas are incorporated into a MIMO handset system as an individual antenna radiating element.

To resolve the isolation dilemma, some techniques have been developed [8–10]. Slots etched on the ground plane have been utilized as an equivalent band-stop filter to improve isolation [8], while mushroom-like electromagnetic band gap (EBG) structures have also been employed [9]. In addition, decoupling and matching networks have been proposed [10]. While the aforementioned methods effectively improve isolation performance, the additional decoupling structures require extra space and increase of the complexity of the original MIMO antenna. Furthermore, some of these techniques consume a portion of the original radiated energy so that the antenna radiation efficiency is decreased. Therefore,

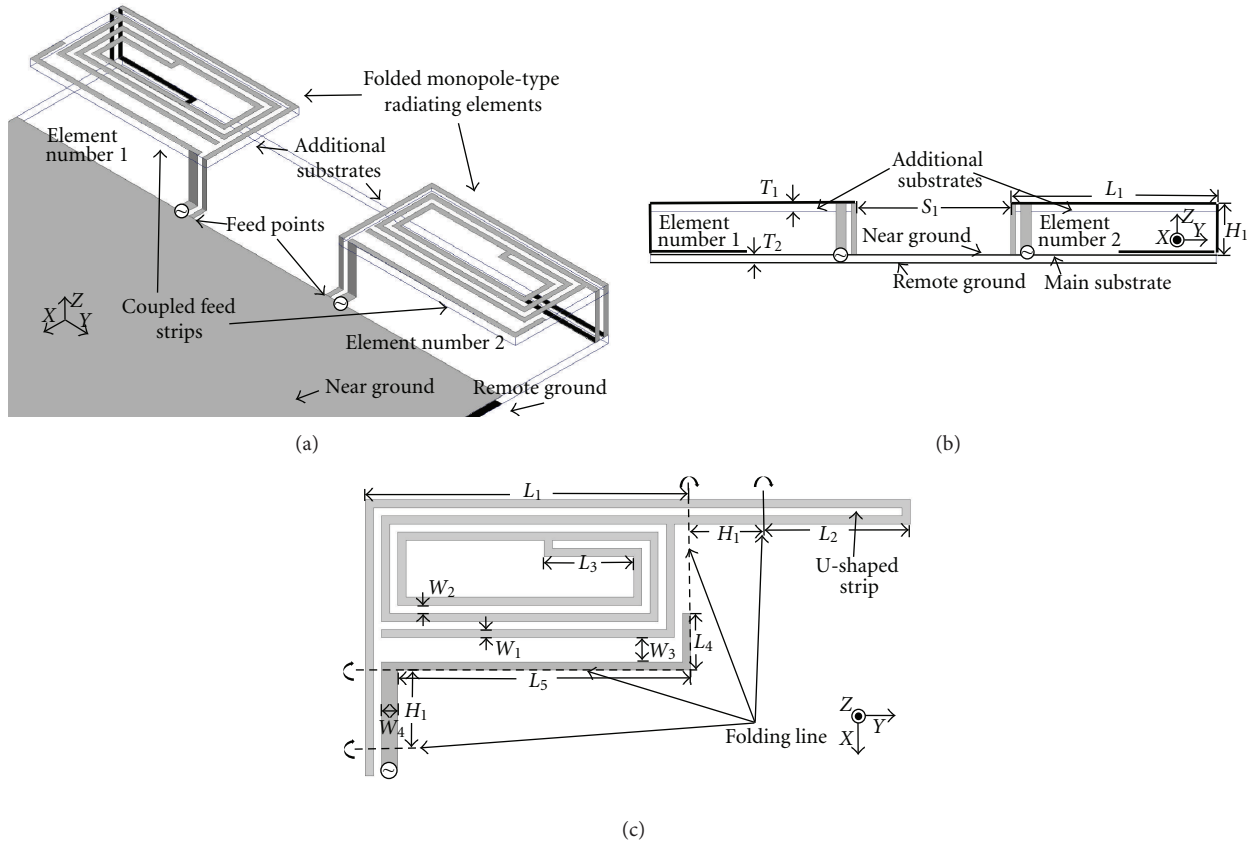


Figure 1: Geometry of the proposed MIMO antenna: (a) perspective view of the antenna, (b) front view of the antenna, and (c) unfolded view of a single antenna element.

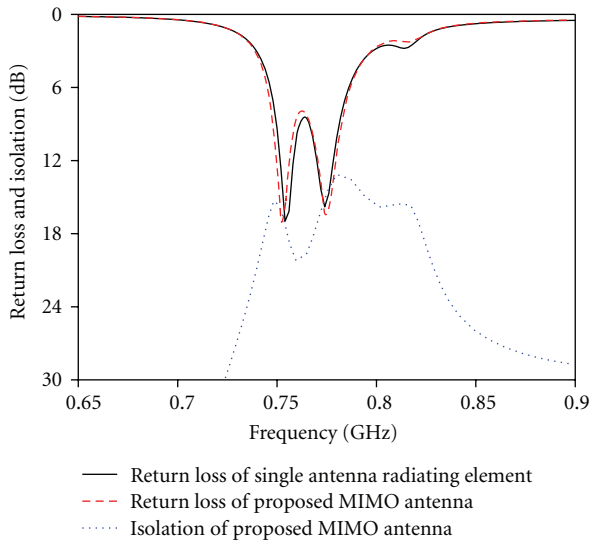


Figure 2: Return loss and isolation characteristics of a single antenna element and the proposed MIMO antenna.

a compact broadband MIMO antenna satisfying the isolation requirement without any additional decoupling structure is preferred.

In this paper, a compact monopole-type MIMO antenna using coupled feed is proposed to cover LTE band 13. The antenna utilizes a Z-shaped capacitive coupled feed strip instead of normal direct number feed structures (i.e., directly connecting the feed point with the main radiating section) to effectively modify antenna impedance matching and maintain isolation. The proposed MIMO antenna has a simple compact monopole-type radiating structure and exhibits broadband properties covering the targeted band. In addition, the MIMO antenna yields good isolation performance without the use of an extra isolation enhancement element.

## 2. Antenna Design and Analysis

*2.1. Antenna Structure.* The geometry of the proposed MIMO antenna is shown in Figure 1. The antenna consists of two identical antenna elements (element number 1 and element number 2) that are symmetrically situated along the $x$-axis. Each antenna element contains a Z-shaped coupled feed strip and a folded monopole-type radiating element. The antenna elements are placed on additional FR4 substrates ($\varepsilon_r = 4.4$) with dimensions of 20 mm × 10 mm × 0.8 mm. Since the total space available for the MIMO antenna is 55 mm × 12 mm × 5 mm, the dimensions of each antenna element are limited to 20 mm × 10 mm × 5 mm. The separation distance

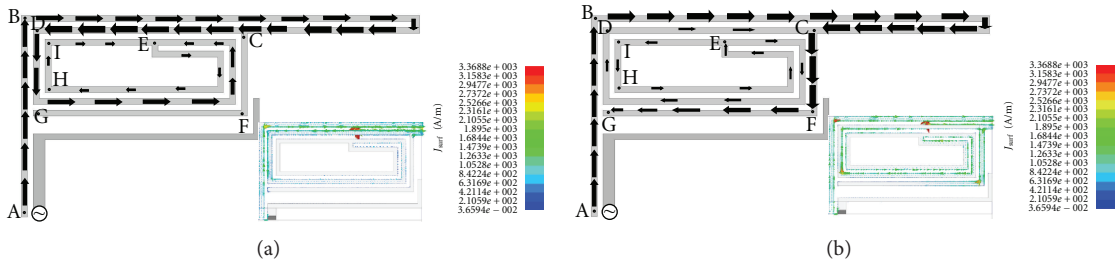


(a) (b)

Figure 3: Current distributions at (a) 0.752 GHz and (b) 0.776 GHz.

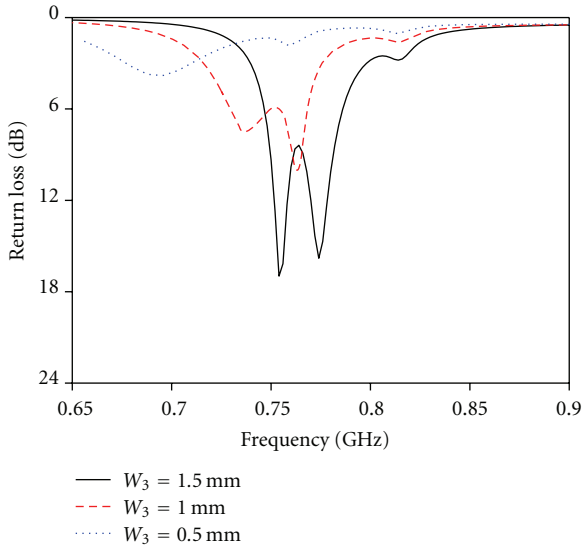


Figure 4: Return loss of the antenna with respect to a variation in the separation width between the radiating element and the coupled feed strip ($W_3$).

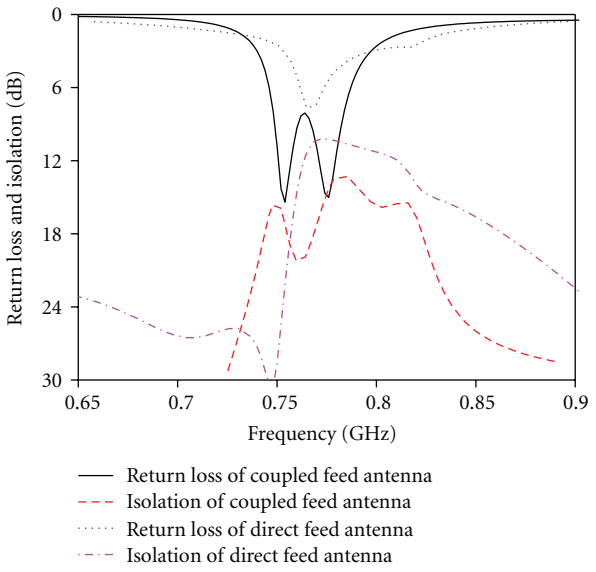


Figure 6: Return loss and isolation characteristics of the proposed main folded monopole element with either a coupled feed structure or a direct feed structure.

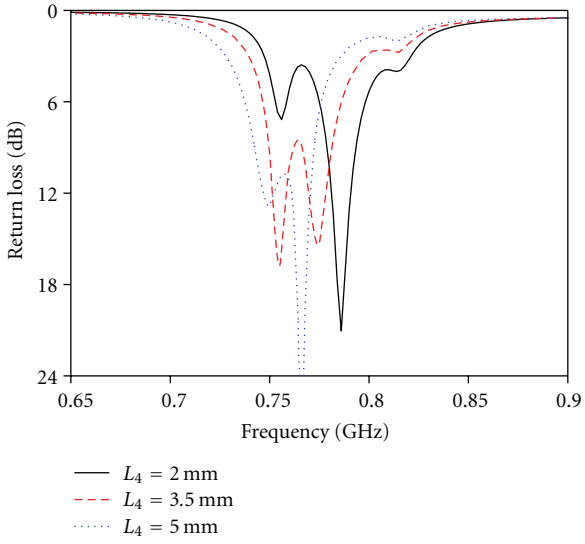


Figure 5: Return loss of the antenna with respect to a variation in the coupled feed strip length ($L_4$).

between the two antenna elements ($S_1$) is 15 mm. As shown in Figure 1(b), other electronic components in the handset are simplified as near and remote grounds, which are placed on both sides of the main FR4 substrate. The near ground, where the feed points are connected, is located on the upper surface, while the remote ground is placed on the lower surface. The dimensions of the main substrate are 55 mm × 100 mm × 0.8 mm, and the areas of both ground planes are 55 mm × 88 mm. The unfolded structure of a single antenna element is illustrated in Figure 1(c). The meander strips in the folded monopole-type radiating element have a width ($W_1$) of 0.5 mm. The separation between the two adjacent strips ($W_2$) is also set to be 0.5 mm. Two U-shaped strips are etched on the upper surface of the main substrate with a length ($L_2$) of 8.5 mm. The separation distance between the radiating element and the coupled feed strip ($W_3$) is 1.5 mm, while the total length of the Z-shaped coupled feed strip ($H_1 + L_5 + L_4$) is set to be 26.5 mm.

The optimized design parameters for the proposed MIMO antenna are summarized in Table 1.

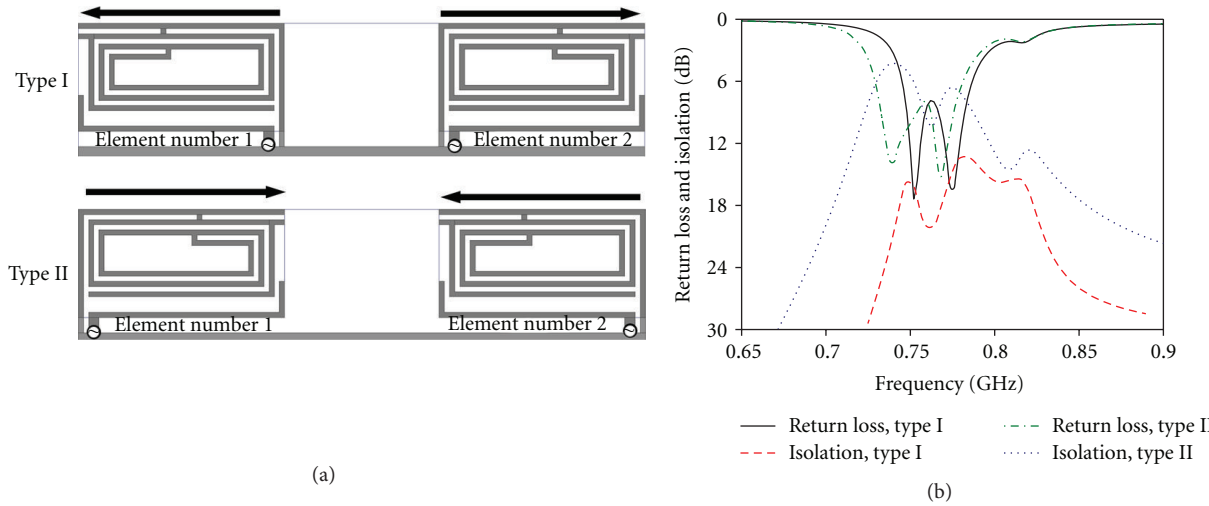


FIGURE 7: Return loss and isolation characteristics of the antenna with respect to a variation in the antenna element arrangement: (a) types of antenna arrangements and (b) return loss and isolation characteristics.

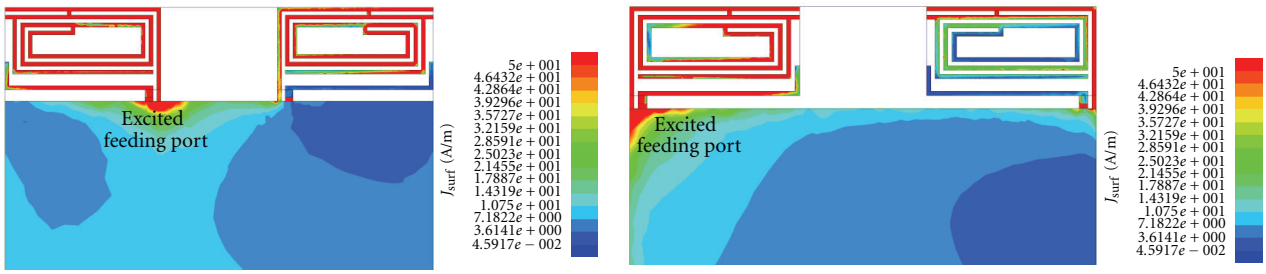


FIGURE 8: Current distributions at 0.752 GHz: (a) type I and (b) type II.

TABLE 1: Optimized design parameters of the proposed antenna.

| Parameter | $L_1$ | $L_2$ | $L_3$ | $L_4$ | $L_5$ | $H_1$ | $S_1$ | $W_1$ | $W_2$ | $W_3$ | $W_4$ | $T_1$ | $T_2$ |
|---|---|---|---|---|---|---|---|---|---|---|---|---|---|
| Value (mm) | 20 | 8.5 | 5.5 | 3.5 | 18 | 5 | 15 | 0.5 | 0.5 | 1.5 | 1 | 0.8 | 0.8 |

*2.2. Antenna Analysis.* The simulated return loss and isolation of the proposed MIMO antenna and a single antenna element are compared in Figure 2. The return loss characteristics are almost the same in LTE band 13 for both cases. The results show that the proposed MIMO antenna has broadband properties and good isolation characteristics over the desired frequency band. Moreover, both the proposed MIMO antenna and the single antenna element have extra impedance resonances around 0.82 GHz due to the resonance of the remote ground at this frequency.

As shown in Figure 2, the proposed folded main radiating element has two nearby resonances that are excited separately at frequencies of 0.752 GHz and 0.776 GHz to achieve broadband characteristics. To explain how a single compact radiating element supports two nearby resonances to satisfy the broadband requirement, the surface current distributions on the main folded monopole element for two resonance frequencies were simulated; the results are shown in Figure 3. The main radiating element supports two monopole modes (first order). The lower-frequency monopole mode at 0.752 GHz has current flowing along path A-B-C-D-E-H-I-E, while the upper-frequency monopole mode at 0.776 GHz has current that mainly flows along path A-B-C-F-G.

The use of only the folded monopole element supporting different modes is not sufficient to achieve broadband performance. The impedance matching of the proposed MIMO antenna should also be carefully adjusted so as to guarantee a return loss value above a certain targeted level over the desired frequency band (above 6 dB for this case). The coupled feed structure utilized for the MIMO antenna could conveniently modify the input impedance. The simulated return loss of the proposed antenna was investigated in order demonstrate how the coupled feed structure satisfies impedance matching.

The return loss of the proposed antenna with respect to a variation in the separation distance between the radiating element and the coupled feed strip ($W_3$) is shown in Figure 4. As $W_3$ decreases, the value of the capacitance induced by

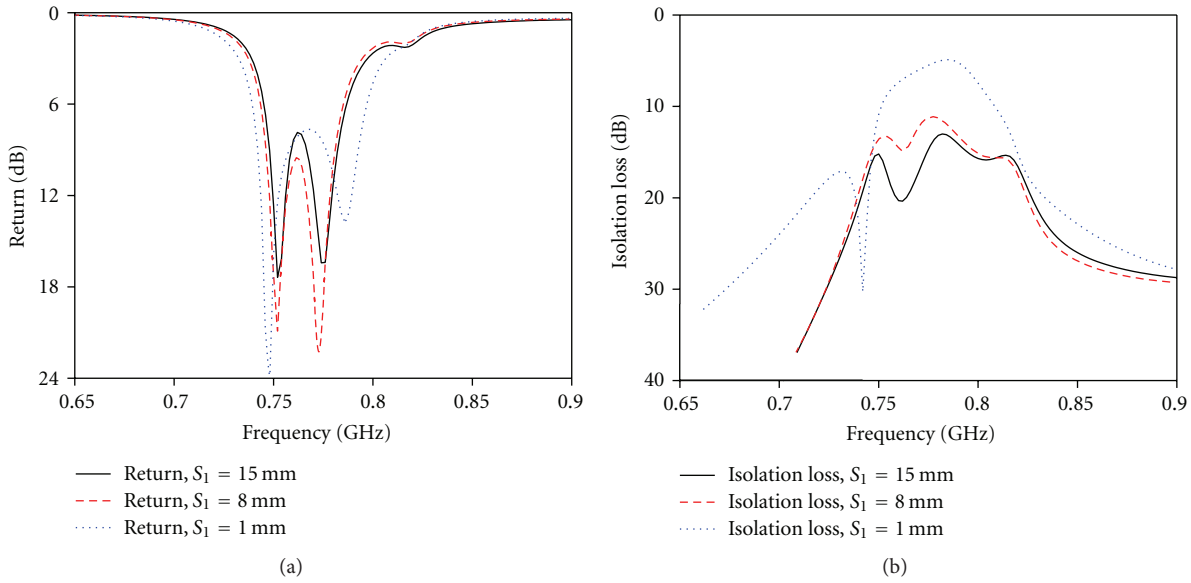


FIGURE 9: Return loss and isolation of the antenna with respect to a variation in distance between different radiating elements ($S_1$): (a) return loss and (b) isolation.

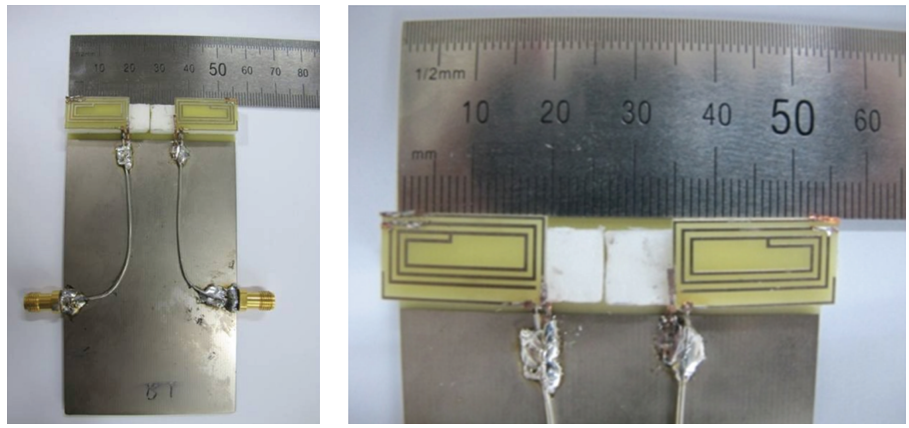

FIGURE 10: Photographs of the fabricated antenna.

capacitive separation increases. The resonant frequencies of both the lower and upper monopole modes shift in the lower frequency direction, while the impedance matching deteriorates over the entire band.

The return loss of the proposed antenna with a variation in the coupled feed length ($L_4$) is shown in Figure 5. A variation in $L_4$ could also change the input impedance of the MIMO antenna. When $L_4$ increases, the impedance matching improves and the resonant frequency shifts in the lower frequency direction.

In addition to the bandwidth, the isolation characteristic is another key parameter to evaluate the performance of a MIMO antenna. The aforementioned coupled feed structure should also allow good isolation to be maintained.

The return loss and isolation characteristics of the proposed main folded monopole element with either a coupled feed structure or a direct feed structure are compared in Figure 6. When compared to the antenna with a direct feed structure, the proposed antenna with a coupled feed strip has better isolation characteristics. The effective additional capacitance, which is brought by the capacitive slot between the coupled feed and the radiating element, could improve the isolation. The coupled feed structure not only effectively maintains good isolation but also overcomes the narrower bandwidth and inferior impedance matching associated with the direct feed structure.

To further investigate possible improvements in the isolation characteristics, we analyzed the effect of the antenna element arrangement on the overall antenna performance. The return loss and isolation characteristics of the proposed antenna with respect to a variation in the antenna element arrangement are shown in Figure 7. In type I configuration, the two main radiating elements have a back-to-back arrangement with a feeding point located around the middle

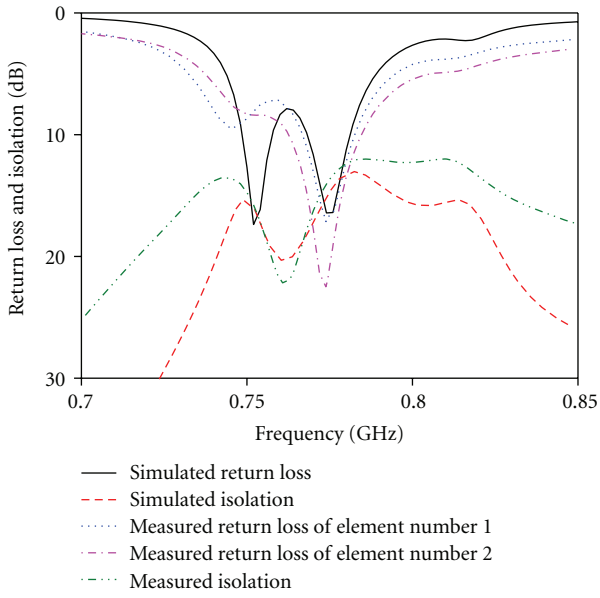


Figure 11: Simulated and measured return loss and isolation characteristics of the proposed MIMO antenna.

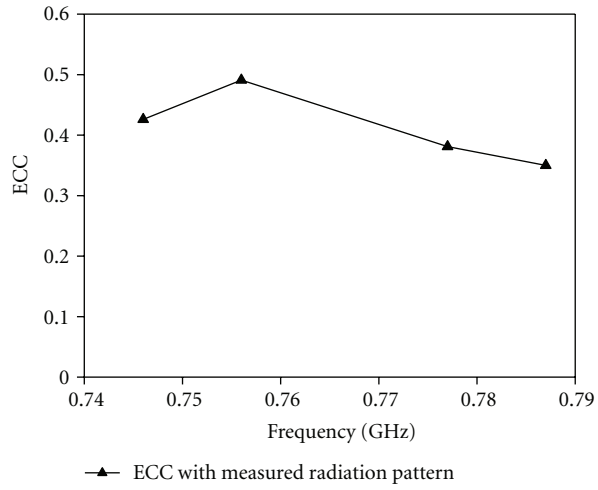


Figure 12: Measured ECC characteristic.

portion of the top edge of the ground plane. In type II arrangement, the two main radiating elements have a face-to-face configuration with a feeding point located around the top corner of the ground plane. When compared to type I (the proposed MIMO antenna in this paper) arrangement, type II configuration yields much worse isolation, even though the bandwidth improves. The reason for the better isolation performance of type I arrangement is that the main radiation direction of each element is away from each other. However, type II arrangement induces stronger current distribution around the other feeding port. The current distributions of antenna for different antenna element arrangement are shown in Figure 8. Therefore, coupling between the radiating elements of type I arrangement is weaker than that of type II configuration.

The return loss and isolation of proposed antenna with respect to a variation in distance between different radiating elements ($S_1$) are shown in Figure 9. Separating antenna elements apart from each other is a natural idea to obtain good isolation. As the distance between different radiating elements reduces from 15 mm to 1 mm, the isolation reduces from above 12 dB to above 4 dB. However, the bandwidth improves because of the strong coupling between different antenna elements.

Due to the limitations imposed on the antenna size, bandwidth, and isolation, the efficiency of proposed antenna is not very high. However, it is not determinant reason that better isolation is obtained. As shown in Figure 7, the arrangement of antenna radiating element is modified without changing any element structure. The isolation decreases from 12 dB to 5 dB. It is also shown in Figure 8 that separating antenna elements apart from each other could improve isolation. Without proper antenna design, the MIMO antenna with low efficiency could still have bad isolation.

The geometry of the proposed antenna was determined and analyzed using a commercial simulation tool, Ansoft HFSS V.13.0.

## 3. Measurements

Photographs of the fabricated antenna are shown in Figure 10. Additional foam (Rohacell, $\varepsilon_r = 1.05$) was inserted into the main substrate so as to ensure that the MIMO antenna was mechanically robust.

The simulated and measured return loss and isolation characteristics of the designed antenna are compared in Figure 11. The measured results confirm that the proposed antenna achieves the 6 dB bandwidth of 55 MHz (0.735 GHz–0.79 GHz), which fully covers LTE band 13. The proposed antenna has isolation above 12 dB over the entire desired frequency band. The differences between the simulated and measured results are mainly due to error produced during the manufacturing.

The ECC of proposed MIMO antenna is shown in Figure 12. The ECC is calculated using measured radiation pattern [11]. The value of ECC is lower than the required maximal level of 0.5, which makes the proposed antenna useful for a MIMO system.

The radiation patterns measured at 0.756 GHz and 0.777 GHz are shown in Figure 13; 3D views of the total radiation patterns from element number 1 and element number 2 were measured and plotted. For element number 1, the radiation efficiency is 23%, and the peak realized gain is −4.71 dBi at 0.756 GHz. At 0.777 GHz, the radiation efficiency of element number 1 is 27.5%, and the peak realized gain is −3.55 dBi. For element number 2, the radiation efficiency is 24%, and the peak realized gain is −4.44 dBi at 0.756 GHz. At 0.777 GHz, the radiation efficiency of element number 2 is 25.5%, and the peak realized gain is −4.11 dBi.

## 4. Conclusion

In this paper, a compact MIMO antenna was designed to operate in LTE band 13. Although the volume of the MIMO

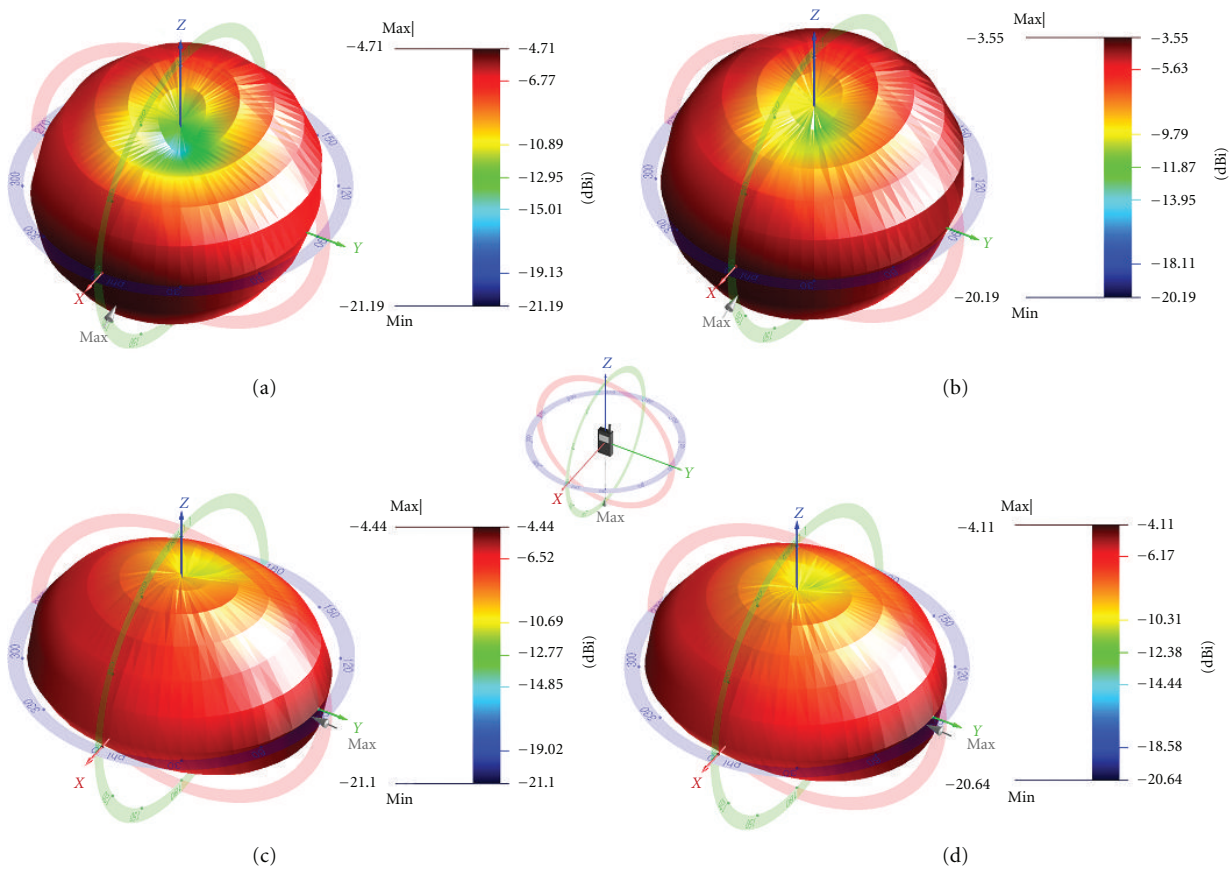


Figure 13: Measured radiation patterns: (a) element number 1 at 0.756 GHz, (b) element number 1 at 0.777 GHz, (c) element number 2 at 0.756 GHz, and (d) element number 2 at 0.777 GHz.

antenna and the separation between different antenna elements are extremely limited, the results confirm that the proposed antenna achieves the 6 dB bandwidth of 55 MHz (0.735 GHz–0.79 GHz), which covers the targeted band. The proposed antenna also has isolation above 12 dB over the entire frequency band. Furthermore, the ECC calculated using measured radiation pattern was verified to be smaller than 0.5. These properties make the proposed MIMO antenna suitable for LTE mobile applications.

## Acknowledgment

This work was supported by a National Research Foundation of Korea (NRF) Grant funded by the Korean government (MEST) (no. 2012-0005655).

## References

[1] D. Astély, E. Dahlman, A. Furuskär, Y. Jading, M. Lindström, and S. Parkvall, "LTE: the evolution of mobile broadband," *IEEE Communications Magazine*, vol. 47, no. 4, pp. 44–51, 2009.

[2] R. G. Vaughan and J. B. Andersen, "Antenna diversity in mobile communications," *IEEE Transactions on Vehicular Technology*, vol. 36, no. 4, pp. 149–172, 1987.

[3] H. Li, Y. Tan, B. K. Lau, Z. Ying, and S. He, "Characteristic mode based tradeoff analysis of antenna-chassis interactions for multiple antenna terminals," *IEEE Transactions on Antennas and Propagation*, vol. 60, no. 2, 2012.

[4] K. L. Wong, Y. C. Lin, and T. C. Tseng, "Thin internal GSM/DCS patch antenna for a portable mobile terminal," *IEEE Transactions on Antennas and Propagation*, vol. 54, no. 1, pp. 238–241, 2006.

[5] W. Y. Lee, Y. S. Jeong, S. H. Lee, J. R. Oh, K. S. Hwang, and Y. J. Yoon, "Internal mobile antenna for LTE / DCN / US-PCS," in *Proceedings of the Asia-Pacific Microwave Conference (APMC '10)*, pp. 2240–2243, December 2010.

[6] C. H. Chang and K. L. Wong, "Printed λ/8-PIFA for penta-band WWAN operation in the mobile phone," *IEEE Transactions on Antennas and Propagation*, vol. 57, no. 5, pp. 1373–1381, 2009.

[7] C. T. Lee and K. L. Wong, "Planar monopole with a coupling feed and an inductive shorting strip for LTE/GSM/UMTS operation in the mobile phone," *IEEE Transactions on Antennas and Propagation*, vol. 58, no. 7, pp. 2479–2483, 2010.

[8] C. Y. Chiu, C. H. Cheng, R. D. Murch, and C. R. Rowell, "Reduction of mutual coupling between closely-packed antenna elements," *IEEE Transactions on Antennas and Propagation*, vol. 55, no. 6, pp. 1732–1738, 2007.

[9] D. Sievenpiper, L. Zhang, R. F. Jimenez Broas, N. G. Alexöpolous, and E. Yablonovitch, "High-impedance electromagnetic surfaces with a forbidden frequency band," *IEEE Transactions on Microwave Theory and Techniques*, vol. 47, no. 11, pp. 2059–2074, 1999.

[10] S. C. Chen, Y. S. Wang, and S. J. Chung, "A decoupling technique for increasing the port isolation between two strongly coupled antennas," *IEEE Transactions on Antennas and Propagation*, vol. 56, no. 12, pp. 3650–3658, 2008.

[11] J. F. Li, Q. X. Chu, and T. G. Huang, "A compact wideband MIMO antenna with two novel bent slits," *IEEE Transactions on Antennas and Propagation*, vol. 60, no. 2, pp. 482–489, 2012.